Rapid growth and properties of large-aperture 98%-deuterated DKDP crystals

Xumin Cai[1,2], Xiuqing Lin[1], Guohui Li[1], Junye Lu[1], Ziyu Hu[1,3], and Guozong Zheng[1]

[1]*Fujian Institute of Research on the Structure of Matter, Chinese Academy of Sciences, Fuzhou 350002, China*

[2]*University of Chinese Academy of Sciences, Beijing 100049, China*

[3]*College of Chemistry, Fuzhou University, Fuzhou 350116, China*

Abstract
In this paper, a highly deuterated potassium dihydrogen phosphate (DKDP) crystal with sizes up to 318 mm × 312 mm × 265 mm was grown by the rapid-growth method. The synthesis tank device was specially designed to synthesize a higher deuterium concentration and high-purity DKDP solution. The deuterium content of the as-grown crystal, which was 97.9%, was determined by two methods, including infrared (IR) spectroscopy and thermo-gravimetric analysis (TGA) measurements. The performances of the 97.9% DKDP crystal, including transmission, absorption coefficient, and laser-induced damage threshold (LIDT) were measured. The results indicate that, in the near-infrared band, the transmission of the 97.9% DKDP crystal is higher than that of KDP and 70% DKDP crystals, and the absorption coefficient is lower. The LIDT of the crystal reached 23.2 J · cm^{-2} (R-on-1, 1064 nm, 3 ns), which meets the engineering requirements for use in optical applications.

Keywords: DKDP crystal; large aperture; highly deuterated DKDP; rapid growth

1. Introduction

Deuterated potassium dihydrogen phosphate (DKDP) crystals are optical materials with excellent properties, such as high transmittance, high electro-optic coefficient and high laser damage threshold, which are widely used for frequency conversion and as electro-optical *Q*-switching crystals in inertial confinement fusion (ICF) projects[1–3]. In particular, DKDP crystals can grow to very large apertures, up to 900 mm by the water solution method[2]. Due to a hydrogen atom being replaced by a deuterium atom, DKDP crystals have a few differences in performance compared with potassium dihydrogen phosphate (KDP) crystals, including a weak stimulated Raman scattering (SRS) effect[4–6] and a low half-wave control voltage, which is about half that of KDP crystals[7]. As the number of deuterium atoms increases, the electro-optic properties become better[8]. The ICF project chooses large-aperture, highly deuterated crystals as electro-optic switch materials[9]. However, the growth of large-size, 98%-deuterated DKDP crystals faces many difficulties, such as disturbance of the monoclinic DKDP crystal during the growth of the tetragonal DKDP

crystal, hydrogen–deuterium exchange, and the need for expensive heavy water[8, 10]. To date, there have been very few reports on the growth of highly deuterated DKDP crystals.

The traditional temperature-reduction method for producing crystals has been widely used to grow large-size, highly deuterated DKDP crystals, which requires a long period of more than one year[2, 11, 12]. It is difficult to supply enough DKDP crystals by the traditional method, so a rapid-growth technology is being urgently studied for highly deuterated DKDP crystals. In 2014, Zhang *et al.*[8] reported that DKDP crystals with a deuterium content of 98% and sizes of 100 mm × 105 mm × 96 mm were successfully grown by point-seed technology. The tetragonal-to-monoclinic solubility transition can be avoided by the rapid-growth technique[10]. It is essential that a rapid-growth method is used for the growth of highly deuterated DKDP crystals by the point-seed technique. The growth of large-size, highly deuterated DKDP crystals is affected by many factors[10, 13], such as the need for highly pure raw materials, supersaturation stability, ultrafine filtration, the rate of hydrogen–deuterium exchange, and the disturbance of the monoclinic crystal. At present, large-scale, high-quality, highly deuterated DKDP crystals are urgently needed for

---

Correspondence to: G. Zheng, 155 West Yangqiao Road, Fuzhou 350002, China. Email: zhengguozong@fjirsm.ac.cn

Table 1. Concentration of the main metallic ionic impurities in P_2O_5 raw material (ppb, parts per billion).

Element	Concentration (ppb)	Element	Concentration (ppb)
Al	46.81	Pb	9.02
As	32.74	Li	10.11
Ba	13.62	Mg	99.08
Co	2.87	Mn	8.32
Cr	10.93	Ni	7.51
Cu	13.06	Sr	3.84
Fe	100.82	Zn	25.19

Table 2. Concentration of the main metallic ionic impurities in K_2CO_3 raw material (ppb, parts per billion).
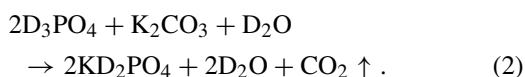
Element	Concentration (ppb)	Element	Concentration (ppb)
Al	123.52	Pb	18.83
As	34.98	Li	39.56
Ba	38.12	Mg	172.84
Co	10.36	Mn	99.75
Cr	55.46	Ni	40.88
Cu	39.65	Sr	20.71
Fe	546.12	Zn	118.23

ICF projects, and researchers are seeking to make a breakthrough. In this paper, we designed a synthesis tank device to prepare a high-deuterium content DKDP crystal solution. A highly deuterated DKDP crystal was grown rapidly by the point-seed technique and continuous filtration, with a size of more than 300 mm, and the crystal quality was examined.

2. Experiment

2.1. Synthesis

Synthesis of the growth solution is the most important factor for the growth of highly deuterated DKDP crystals. The usual procedure was adopted to synthesize the high-deuterium concentration growth solution, which was divided into two steps. First, a phosphorus pentoxide (P_2O_5) reagent of electronic grade (99.9995%) reacted with heavy water of isotopic purity (99.8%). Then, the deuterated ortho-phosphoric acid obtained in the first step reacted with spectrum-pure grade (purity of 99.999%) potassium carbonate (K_2CO_3). The concentrations of the main metallic ionic impurities in the raw materials are listed in Tables 1 and 2. The results in Tables 1 and 2 show that the ingredients are with high purity and can be used for the preparation of the DKDP solution. The reactions are as follows:

$$P_2O_5 + 3D_2O \rightarrow 2D_3PO_4, \tag{1}$$

$$2D_3PO_4 + K_2CO_3 + D_2O$$
$$\rightarrow 2KD_2PO_4 + 2D_2O + CO_2 \uparrow. \tag{2}$$

To avoid hydrogen–deuterium exchange, a synthesis tank device was designed to provide a closed environment for
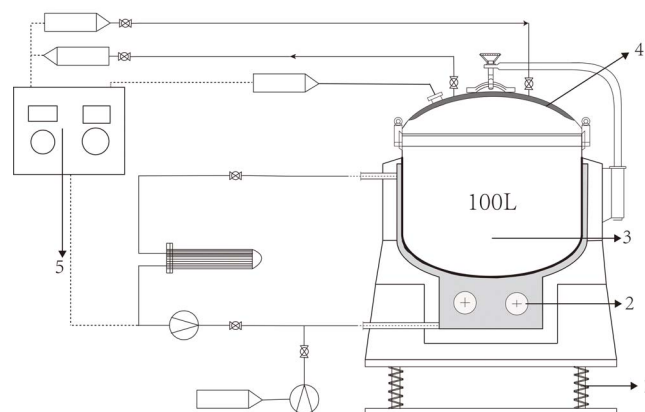
Figure 1. Schematic of the 100 L synthesis tank device. 1, vibrating table; 2, heating unit; 3, synthesis container; 4, cooling system; 5, control system.

these two reactions. The schematic of the synthesis tank device is shown in Figure 1. It includes the synthesis container, a cooling system, a control system and a heating unit, and synthesizes large batches (volume of 100 L) of the growth solution with high purity. The device features highly automated continuous production and high accuracy, and is simple to use compared with the conventional synthesis device.

Before the reactions, K_2CO_3 was dried at 105 °C for more than 12 h to desiccate and reduce the deuterium loss. During the reactions, the tank was placed in a dry environment with a humidity of less than 20%. The saturated temperature of the solution was controlled to 47 °C and the pD value (deuterium ion concentration, pD is similar to pH) was adjusted to 3.9 by calculating the quantity of the raw materials. After the process, the synthesized solution was filtered through a 0.1 μm pump and transferred to the crystallizer.

2.2. Crystal growth

The solution was overheated for more than 72 h in the 500-L standard hold-type crystallizer to avoid spontaneous nucleation. The highly deuterated DKDP crystal was grown rapidly from a 12 mm × 12 mm × 6 mm z-cut point seed in the 500-L crystallizer with a continuous filtration system and a temperature control of ±0.1 °C. The seed, which was free of any visible macroscopic defects, was overheated at 52 °C for 1 h in the growth solution before growth. During the DKDP crystal growth process, the solution was stable without spontaneous nucleation as the temperature decreased from 47 to 38 °C and a rotation rate for the platform was adopted with a speed of about 30 r/min.

The as-grown crystal was 318 mm × 313 mm × 265 mm in size without significant macroscopic defects, with an average growth rate of about 6 mm · day^{-1}, as shown in Figure 2.
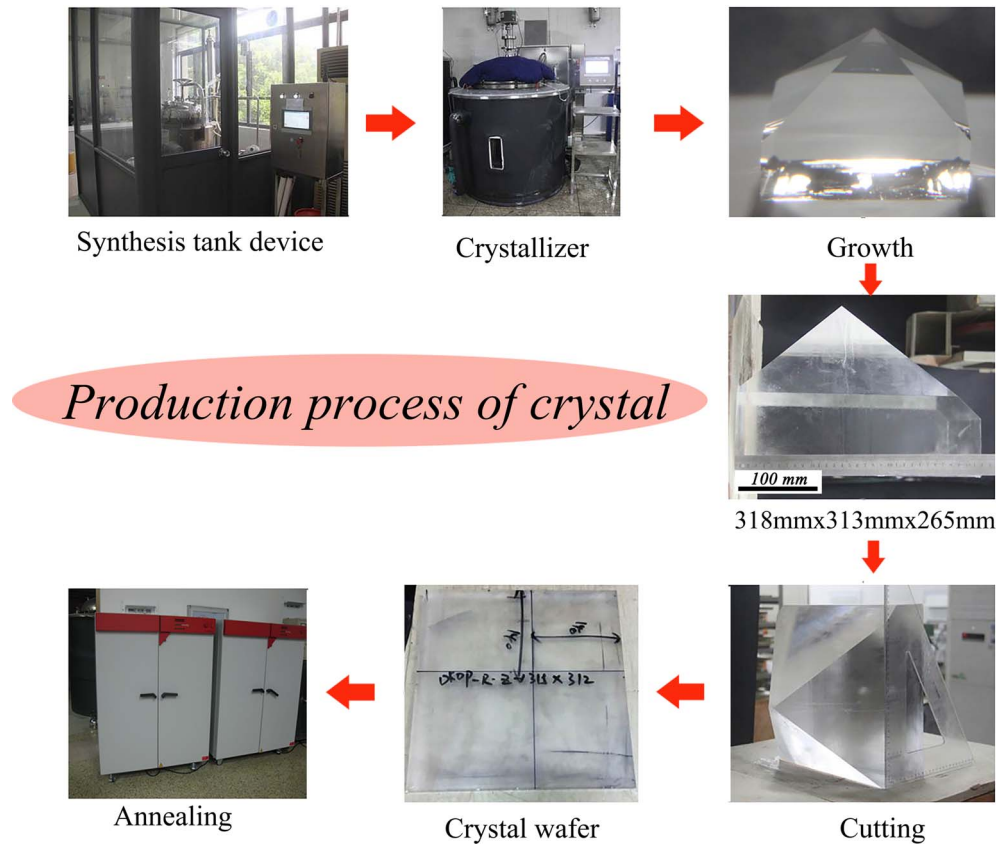
Figure 2. Details of the DKDP crystal production process, including synthesis, growth, cutting and annealing.

After X-ray orientation and *z*-cut, a 315 mm × 312 mm × 12 mm DKDP crystal wafer was obtained, which was annealed at 120 °C for 24 h and used to provide switching devices for the performance examination. Details of the DKDP crystal production process are shown in Figure 2.

2.3. Measurements

Transmittance spectra of the crystal were recorded by a Lambda 950 ultraviolet–visible–near-infrared (UV–vis–NIR) spectrophotometer in the range 200–2000 nm. The spectral resolution of the spectrophotometer was 1 nm. The transmittance value was converted into the absorption coefficient according to the Lambert–Beer law.

The laser-induced damage threshold (LIDT) of DKDP crystals was measured by the Shanghai Institute of Optics and Fine Mechanics. The experimental setup for assessing the damage threshold is shown in Figure 3. The damage threshold was measured by the R-on-1 test. The test wavelength was 1064 nm with a pulse length of 8.8 ns and a 1ω conversion efficiency. For the sake of engineering applications, test results at 8.8 ns were eventually normalized to 3 ns.
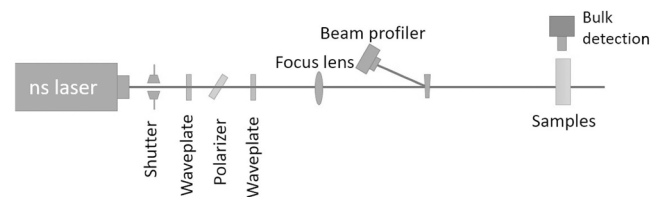

Figure 3. Experimental setup for measuring the LIDT, including shutter, waveplate, polarizer, focus lens, beam profiler and bulk detection.

3. Results and discussion

3.1. Deuterium content of the grown crystal

In DKDP crystals, especially high-deuterium crystal, an accurate measurement of the deuterium concentration is very important. The chemical and physical properties of the hydrogen and deuterium atoms in the DKDP crystal, such as the structural dimensions, bond lengths and bond angles, are closely related to the deuterium content of DKDP crystals[14, 15]. There are multiple methods available to determine the deuterium level. These methods depend on different principles to measure the deuterium concentration[16–20], such as the variation in the ferroelectric

Table 3. Results for the deuterium level of DKDP crystal as assessed from IR spectra.

No.	1	2	3	4	Average
Deuterium level (%)	97.7	98.0	97.9	98.0	97.9

transition

temperature of DKDP, the relationship between the deuterium concentration and the Raman shift of the PO_4 vibration peak, the sensitivity of neutrons to hydrogen and deuterium elements, differences in the infrared spectra of hydrogen and deuterium atoms, and the thermo-decomposition of DKDP and KDP crystals, as described in the present literature concerned. These methods have both advantages and drawbacks.

Liu et al.[21] concluded that infrared (IR) spectra present more accurate values for high-deuterium content DKDP crystals. Li et al.[20] concluded that thermo-gravimetric apparatus (TGA) measurement is an accurate method because the residual mass, which is the weight ratio of KPO_3 against DKDP samples, can be obtained from the TG curve of the sample accurately using thermo-gravimetric apparatus. The TGA method has the advantages of simple manipulation, low sample consumption (30–90 mg) and a short measurement period (about 2.5 h). Therefore, we used IR spectroscopy and TGA measurements to determine the deuterium content of the as-grown DKDP crystal in this study.

The as-grown DKDP crystal was z-cut to obtain samples with sizes of 10 mm × 10 mm × 20 mm. These samples were obtained from prismatic and pyramid regions of the crystal, with the location of the samples shown in Figure 4. The samples were then lapped and polished without any coating. The IR spectra were measured in the range 200–1800 nm for 20 mm thick z-cut specimens. The recorded spectra are shown in Figure 5. Based on years of experimental results, a database has been established for the deuterium level and the optical transmission (@1550 nm). This database is constantly revised based on theory (Fresnel losses) and experiments, and the results of the database are reliable. Using this database, the transmission (@1550 nm) can be converted into the deuteration levels which are shown in Table 3. From Table 3, the deuterium concentrations of samples 2 and 4 are a little higher than those of samples 1 and 3. However, the difference is not significant, thus showing excellent homogeneity in the deuterium level. The average value of the deuterium content is 97.9%.

To accurately measure the degree of deuteration of crystals, we also used the TGA method to determine the deuterium concentration of the as-grown DKDP crystal. Samples of approximately 80 mg from different parts of the as-grown DKDP crystal were selected for measurement of the thermo-gravimetric curve. Samples 1 and 2 were taken from the pyramid and prismatic regions of the crystal, respectively, with the location of each sample being shown in Figure 6.
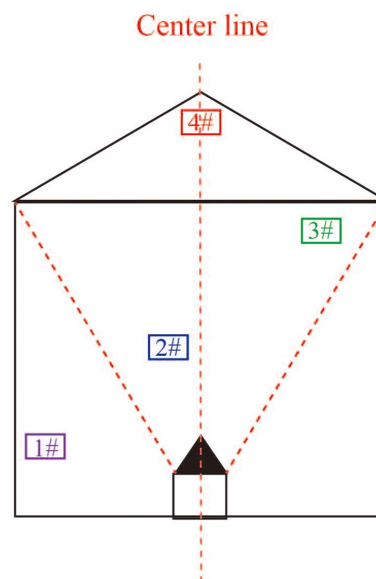

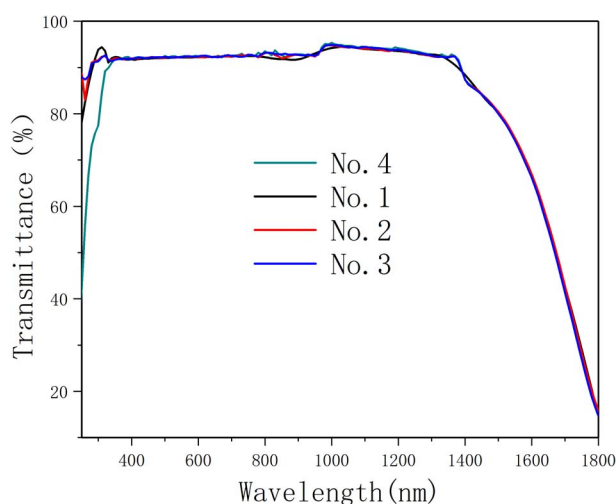**Figure 4.** Locations of the samples used in infrared (IR) spectra measurements.

Figure 5. IR spectra. The recorded spectra were measured by a spectrophotometer in the range 200–1800 nm.

The TG curves of the DKDP crystals are shown in Figure 7. The results for the residual weight of DKDP crystals are listed in Table 4. Equation (3) was used to calculate the deuterium concentration of the DKDP crystals, as follows[20]:

$$D = \left(\frac{58.699}{\alpha} - 67.62 \right) \times 100\%, \qquad (3)$$

where D is the deuterium level of the DKDP crystal and α is the residual mass. The average value for the degree of deuteration of crystals is 96.94% by the TGA method. The deuterium level of sample 1 from the pyramid region is a little higher than that of sample 2 from the prism region. The
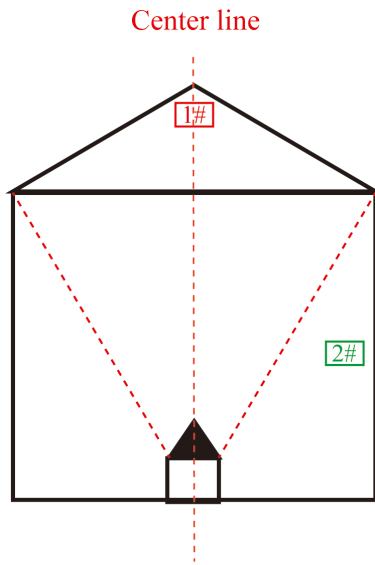
Figure 6. Locations of the samples used in TGA measurements.

Figure 7. Thermo-gravimetric curve of DKDP crystals. The red curve represents the heating curve and the two black curves represent the TG curve of DKDP.

deuterium concentration of the pyramid region is higher than that of the prismatic region, but the difference is not obvious. From the results for the deuterium level assessed both by IR spectroscopy and TGA measurements, it is clear that the as-grown crystal possesses good homogeneity in its deuterium concentration. The results obtained from IR spectroscopy are slightly higher than those from TGA measurements. IR spectroscopy is more suitable for measuring highly deuterated DKDP crystals – therefore, the value of 97.9% measured by IR spectroscopy is used as the measured value of the deuteration level of the as-grown DKDP crystal.

The effective distribution coefficient of deuterium is described by the following exponential equation[17]:

$$k_{\mathrm{eff}} = 0.68 \exp(0.00382M), \qquad (4)$$

where M is the mole fraction of deuterium in the solution and k_{eff} is the effective distribution coefficient of deuterium. The deuterium concentration of the mother solution is about 99%. Hence, the deuterium level of the as-grown crystal is about 98% according to the exponential equation. Two methods were used to determine the deuterium content of the as-grown DKDP crystals: IR spectroscopy and TGA measurements of the deuterium concentration give 97.9% and 96.9%, respectively, which are lower than the value calculated by the exponential equation. Because of the effect of hydrogen–deuterium exchange, the deuterium concentration of the solution decreased during the growth of the DKDP crystal. However, in this experiment, it can be ascertained that the deuterium level of the as-grown DKDP crystal was more than 96% with both measuring methods, and the as-grown crystal is a highly deuterated DKDP crystal as used in the optical components.
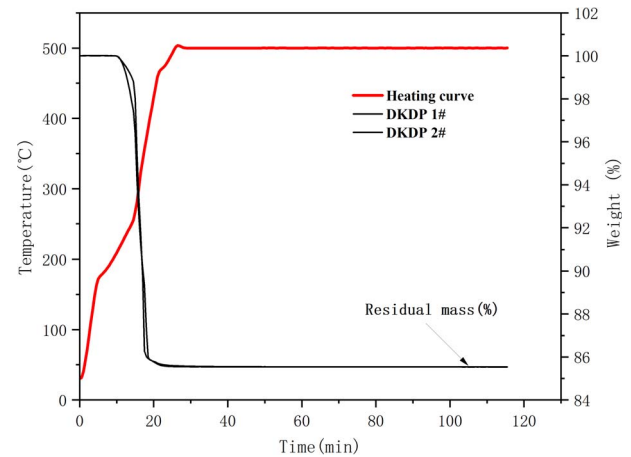
Table 4. Results of the residual mass and deuterium level of DKDP.

Samples	Residual mass (%)	Deuterium level (%)
DKDP-1#	85.53191	97.22
DKDP-2#	85.53906	96.65
Average	85.53549	96.94

3.2. Optical properties of DKDP crystal

Highly deuterated DKDP crystals with excellent optical properties are widely used for optical applications. The absorption coefficient of DKDP crystals is a significant parameter used to assess the optical properties and quality of crystals, which was measured from the transmission spectra in this paper. Samples of 15 mm × 15 mm were *z*-cut from the pyramid region of the large DKDP crystal (the schematic cutting diagram is shown in Figure 8). The samples were processed into plates of 10 mm thickness and the transmitting faces of the crystal were fine polished without coating by a fly-cutting machine tool until they were free of scratches and the sample became transparent. Optical transmission spectra recorded by a spectrophotometer (Lambda 950) in the range 200–2000 nm at room temperature are shown in Figure 9. We also measured the transmission spectra of 70% DKDP and KDP crystals under the same conditions.

The highly deuterated DKDP crystal was used in electro-optical *Q*-switch materials for the near-infrared waveband (such as at 1053 nm or 1064 nm). It is observed from Figure 9 that, in the near-infrared band, the transmittance of 97.9% deuterated DKDP crystal is significantly higher than those of 70% DKDP and KDP crystals because the introduction and concentration of deuterium atoms weakened the infrared absorption caused by vibrations of the O-H band. Reference [22] considered the transmittance of the crystal at 355 nm was more than 88%, which indicated that the optical performance of the as-grown
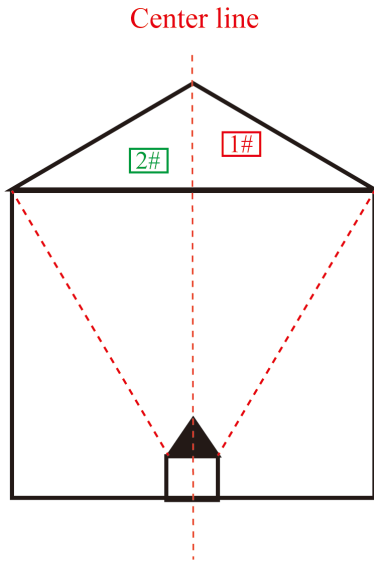
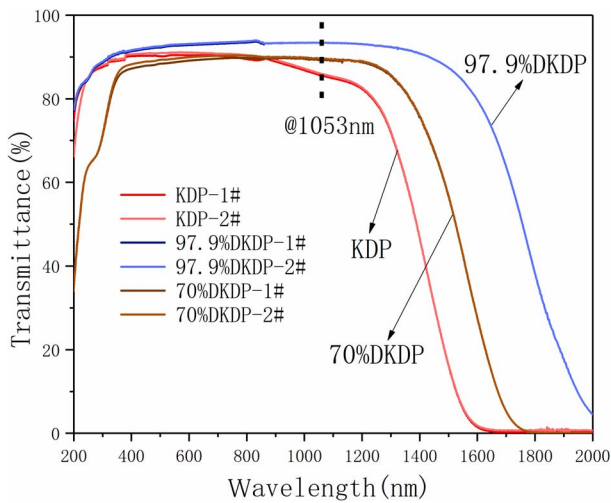**Figure 8.** Schematic cutting diagram for the different DKDP samples.

Figure 9. Transmission spectra of different deuterium concentration DKDP and DKP crystals. The blue curve represents 97.9% DKDP crystal, the brown curve represents 70% DKDP and the red curve represents KDP crystal.

Table 5. Results for the transmittance and absorption coefficient with different deuterium levels in DKDP and KDP crystals.

Samples	KDP		70% DKDP		97.9% DKDP	
	T	α_{ac}	T	α_{ac}	T	α_{ac}
	(%)	(cm^{-1})	(%)	(cm^{-1})	(%)	(cm^{-1})
1#	85.645	0.082	89.410	0.031	93.407	0.0052
2#	86.122	0.071	89.707	0.028	93.407	0.0052
Average	85.884	0.077	89.559	0.029	93.407	0.0052

chemical film coating. A spectrophotometer at a wavelength of 1053 nm was used to measure the transmittance of the samples. The transmittance results were 99.76% and 99.82%, which are higher than those of samples without any coating at 1053 nm (Table 5). Therefore, we can conclude that the as-grown highly deuterated DKDP crystal possesses a high transmission.

In accordance with the Lambert–Beer law, the transmittance result is determined by the interface and internal transmittance in the crystal. The relationship can be expressed by the following formula[23]:

$$T_{\text{meas}} = T_{\text{Fresnel}} + T_{\text{bulk}} + T_{\text{Fresnel}}, \tag{5}$$

where T_{meas} is the measured transmittance, T_{Fresnel} is the transmittance of the interface and T_{bulk} is the internal transmittance in the crystal. As light travels through the crystal, Fresnel reflection occurs at every crystal interface. At the crystal interface, the transmittance (T_{Fresnel}) and reflectivity (R_i) have the following relationship:

$$T_{\text{Fresnel}} = 1 - R_i. \tag{6}$$

R_i is estimated from the refractive index, as follows:

$$R_i = \left(\frac{1-n}{1+n}\right)^2. \tag{7}$$

In accordance with the Lambert–Beer law,

$$I_o = I_i e^{-\alpha_{ac}L}, \tag{8}$$

$$T_{\text{bulk}} = \frac{I_o}{I_i}. \tag{9}$$

Hence, one obtains

$$T_{\text{bulk}} = I_i e^{-\alpha_{ac}L}. \tag{10}$$

Using Equations (5) and (6) directly yields

$$T_{\text{bulk}} = \frac{T_{\text{meas}}}{(T_{\text{Fresnel}})^2} = \frac{T_{\text{meas}}}{(1-R_i)^2}. \tag{11}$$

crystal was pretty good. In Figure 9, the transmittance of all 97.9% DKDP sample crystals at 355 nm was more than 89%. The difference in transmission is small between different samples of 97.9% DKDP crystal, thus indicating the good homogeneity in transmission of the pyramidal crystal. To accurately evaluate the quality of the as-grown crystal, we entrusted Nuclear Physics and Chemistry, China Academy of Engineering Physics to measure the transmittance. They processed the crystal into two 100 mm × 100 mm wafers with a thickness of 10 mm, polished with a
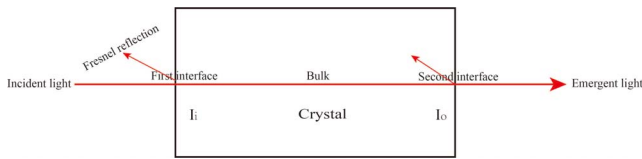
Figure 10. Optical path schematic of the experiment.

Equations (10) and (11) directly yield

$$\frac{T_{\text{meas}}}{(1 - R_i)^2} = I_i e^{-\alpha_{\text{ac}} L}. \tag{12}$$

Hence, one obtains

$$\alpha_{\text{ac}} = \frac{-\ln[T_{\text{meas}}/(1 - R_i)^2]}{L}, \tag{13}$$

where α_{ac} is the absorption coefficient, R_i is the reflectivity and L is the thickness of the DKDP sample. I_i and I_o are the intensities of the incident and emergent light, respectively. n is the refractive index, which is related to the deuterium content of the crystal. A database of the deuterium level and refractive index has been established over many years. The refractive index (n is approximately 1.4) was estimated from the deuterium content of the crystal using this database. Reflectivity was then calculated from the refractive indices by using Equation (7). The optical path schematic of the experiment is shown in Figure 10. Following calculations, Table 5 is obtained. The average absorption coefficient of 97.9% DKDP crystal is about 0.0052 at 1053 nm, which is less than for the 70% DKDP and KDP crystals.

3.3. LIDT of DKDP crystals

The LIDT is one of the most important properties of DKDP crystals and is a measure of the resistance to laser damage. As-grown DKDP crystal wafers with dimensions of 50 mm × 50 mm × 10 mm were cut along the *z*-axis direction from the pyramid region of the crystal and polished thoroughly without any coating. These crystal wafers were then measured using an R-on-1 damage testing facility at a wavelength of 1064 nm with an 8.8 ns pulse width. The LIDT results are recorded in Figure 11 and listed in Table 6. The LIDT values at 3 ns and 10 ns were converted from those at 8.8 ns, which are given in Table 6. From Table 6, the average LIDT of the 97.9% DKDP crystal used for optical applications is 23.2 J·cm^{-2}, which exceeds the engineering requirements of higher than 17 J·cm^{-2} mandated by Nuclear Physics and Chemistry, China Academy of Engineering Physics. With the introduction of deuterium atoms, the LIDT of DKDP crystal decreased[24]. There are many factors that can influence the LIDT of DKDP crystals. To improve the LIDT of highly deuterated DKDP crystals, much work
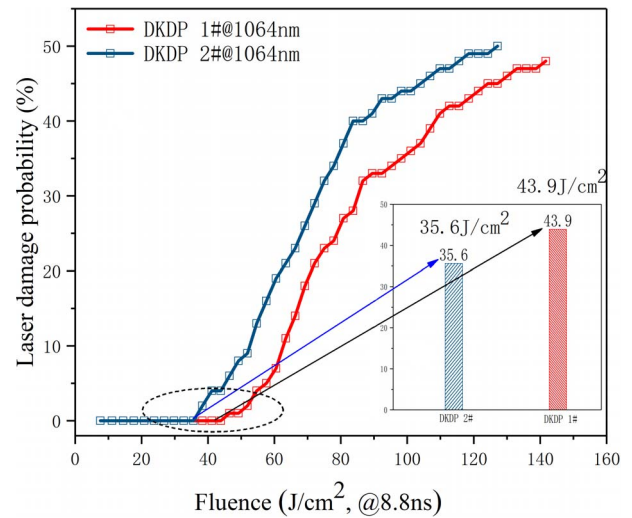

Figure 11. LIDT results. The inset gives the value of LIDT at the inflection point of the curve. The values for samples 1 and 2 are 43.9 J · cm^{-2} and 35.6 J · cm^{-2}, respectively.

Table 6. LIDT results at 8.8 ns, 3 ns and 10 ns.

Samples	LIDT at 8.8 ns (J · cm^{-2})	LIDT at 3 ns (J · cm^{-2})	LIDT at 10 ns (J · cm^{-2})
z-cut-1#	43.9	25.6	46.8
z-cut-2#	35.6	20.8	38.0
Average	39.7	23.2	42.4

has been carried out by researchers. The LIDT of DKDP with a polymethylsiloxane coating reached approximately 28 J · cm^{-2} (1064 nm, 3 ns)[25]. Annealing the DKDP samples led to an improvement of the LIDT[23]. However, the most important method is improving conditions during the growth process to improve the crystal quality. Further research is in process.

4. Conclusions

The properties of a highly deuterated DKDP crystal with sizes of 318 mm × 313 mm × 265 mm grown by the rapid-growth method in a 500-L crystallizer were studied. A synthesis tank device was designed to synthesize a large volume (500 L) of high-purity, highly deuterium content growth solution, which effectively avoids the reduction of deuterium ion concentration and hydrogen–deuterium exchange. The deuterium content of the as-grown DKDP crystal was determined by IR spectroscopy and TGA measurements, giving a value of 97.9%. Transmission and absorption coefficient results confirmed that the as-grown DKDP possessed high optical quality in the near-infrared band. The LIDT of the 97.9% DKDP crystal was 23.2 J · cm^{-2} (1064 nm, 3 ns, R-on-1), which reached the

engineering requirements for use in optical applications. In summary, highly deuterated DKDP crystals with excellent performance, with over 300 mm diameter, can be obtained by the same growth method and equipment.

Acknowledgements

References

1. N. P. Zaitseva, J. J. De Yoreo, M. R. Dehaven, R. L. Vital, K. E. Montgomery, M. Richardson, and L. J. Atherton, J. Cryst. Growth **180**, 255 (1997).
2. N. Zaitseva and L. Carman, Prog. Cryst. Growth Charact. Mater. **43**, 1 (2001).
3. J. J. De Yoreo, A. K. Burnham, and P. K. Whitman, Int. Mater. Rev. **47**, 113 (2002).
4. W. Han, F. Wang, L.-D. Zhou, F.-Q. Li, B. Feng, H.-B. Cao, J.-P. Zhao, S. Li, K.-X. Zheng, X.-F. Wei, M.-L. Gong, and W.-G. Zheng, Opt. Express **21**, 30481 (2013).
5. S. G. Demos, R. N. Raman, S. T. Yang, R. A. Negres, K. I. Schaffers, and M. A. Henesian, Opt. Express **19**, 21050 (2011).
6. W. Han, Y. Xiang, F.-Q. Li, F. Wang, L.-D. Zhou, J.-P. Zhao, B. Feng, K.-X. Zheng, Q.-H. Zhu, X.-F. Wei, W.-G. Zheng, and M.-L. Gong, Appl. Opt. **54**, 4167 (2015).
7. A. M. Vakulenko, N. G. Kryukov, Yu A. Matveets, V. I. Panteleev, Yu V. Senatskii, A. I. Fedosimov, and V. T. Yurov, Soviet J. Quantum Electronics **4**, 76 (1974).
8. L.-S. Zhang, G.-W. Yu, H.-L. Zhou, L. Li, M.-X. Xu, B.-A. Liu, S.-H. Ji, L.-L. Zhu, F.-F. Liu, and X. Sun, J. Cryst. Growth **401**, 190 (2014).
9. P. A. Baisden, L. J. Atherton, R. A. Hawley, T. A. Land, J. A. Menapace, P. E. Miller, M. J. Runkel, M. L. Spaeth, C. J. Stolz, T. I. Suratwala, P. J. Wegner, and L. L. Wong, Fusion Sci. Technol. **69**, 295 (2017).
10. S.-L. Wang, Z.-S. Gao, Y.-J. Fu, A.-D. Duan, X. Sun, C.-S. Fang, and X.-Q. Wang, Cryst. Res. Technol. **38**, 941 (2003).
11. M.-H. Jiang, C.-S. Fang, X.-L. Yu, M. Wang, T.-H. Zheng, and Z.-S. Gao, J. Cryst. Growth **53**, 283 (1981).
12. N. P. Zaitseva, L. N. Rashkovich, and S. V. Bogatyreva, J. Cryst. Growth **148**, 276 (1995).
13. L.-S. Zhang, F. Zhang, M.-X. Xu, Z.-P. Wang, and X. Sun, RSC Adv. **5**, 74858 (2015).
14. D.-W. Fu, W. Zhang, and R.-G. Xiong, Cryst. Growth Des. **8**, 3461 (2008).
15. S. G. Demos, P. DeMange, R. A. Negres, and M. D. Feit, Opt. Express **18**, 13788 (2010).
16. M. A. Yakshin, D. W. Kim, Y. S. Kim, Y. Y. Broslavets, O. E. Sidoryuk, and S. Goldstein, Laser Phys. **7**, 941 (1997).
17. G. M. Loiacono, J. F. Balascio, and W. Osborne, Appl. Phys. Lett. **24**, 455 (1974).
18. T. Huser, C. W. Hollars, W. J. Siekhaus, J. J. De Yoreo, T. I. Suratwala, and T. A. Land, Appl. Spectrosc. **58**, 349 (2004).
19. J. Leroudier, J. Zaccaro, J. Debray, P. Segonds, and A. Ibanez, Cryst. Growth Des. **13**, 3613 (2013).
20. G.-H. Li, G.-B. Su, X.-X. Zhuang, Z.-D. Li, and Y.-P. He, Opt. Mater. **29**, 220 (2006).
21. F.-F. Liu, M.-X. Xu, B.-A. Liu, X.-P. Chen, L. Xie, Y.-H. Xia, C.-W. Wen, L.-S. Zhang, X. Ju, G.-G. Sun, and X. Sun, Opt. Mater. Express **6**, 2221 (2016).
22. X.-Y. Xie, H.-J. Qi, B. Wang, H. Wang, D.-Y. Chen, and J.-D. Shao, J. Cryst. Growth **487**, 45 (2018).
23. D.-T. Cai, Y.-F. Lian, X.-X. Chai, L.-S. Zhang, L.-M. Yang, and M.-X. Xu, Cryst. Eng. Comm. **20**, 7357 (2018).
24. M.-X. Xu, X. Sun, Z.-P. Wang, X.-F. Cheng, S.-T. Sun, L.-L. Ji, Y.-A. Zhao, B.-A. Liu, H. Gao, and X.-G. Xu, Cryst. Res. Technol. **45**, 763 (2010).
25. X.-D. Wang, B.-T. Tian, Y.-Y. Niu, G.-M. Wu, B. Zhou, and J. Shen, Rare Metal Mat. Eng. **45**, 370 (2016).